PLOS ONE

Large Carbon Dioxide Fluxes from Headwater Boreal and Sub-Boreal Streams

Jason J. Venkiteswaran[1,2]*, Sherry L. Schiff[1], Marcus B. Wallin[3]

1 Department of Earth and Environmental Sciences, University of Waterloo, Waterloo, Ontario, Canada, 2 Department of Geography and Environmental Studies, Wilfrid Laurier University, Waterloo, Ontario, Canada, 3 Department of Ecology and Genetics/Limnology, Uppsala University, Uppsala, Sweden

Abstract

Half of the world's forest is in boreal and sub-boreal ecozones, containing large carbon stores and fluxes. Carbon lost from headwater streams in these forests is underestimated. We apply a simple stable carbon isotope idea for quantifying the CO_2 loss from these small streams; it is based only on in-stream samples and integrates over a significant distance upstream. We demonstrate that conventional methods of determining CO_2 loss from streams necessarily underestimate the CO_2 loss with results from two catchments. Dissolved carbon export from headwater catchments is similar to CO_2 loss from stream surfaces. Most of the CO_2 originating in high CO_2 groundwaters has been lost before typical in-stream sampling occurs. In the Harp Lake catchment in Canada, headwater streams account for 10% of catchment net CO_2 uptake. In the Krycklan catchment in Sweden, this more than doubles the CO_2 loss from the catchment. Thus, even when corrected for aquatic CO_2 loss measured by conventional methods, boreal and sub-boreal forest carbon budgets currently overestimate carbon sequestration on the landscape.

Introduction

Boreal and sub-boreal ecozones are large (about 17 million km^2) and about half the world's forest cover [1]. Forests in these zones contain large carbon stores and contribute significant fluxes in the global carbon budget [2]. Part of the carbon fixed from the atmosphere by forests is returned to the atmosphere via aquatic surfaces [3–6]. In the past, this flux has been ignored in the construction of carbon budgets for forested watersheds and is now predicted to be higher than expected [7]. In Sweden, annual estimates of carbon sequestration in forests are 10% lower if aquatic carbon losses are included [8]; similar amounts are expected for Norway [9]. In the USA, stream and river CO_2 loss may be five times greater than previously thought [10]. The difficulty in accounting for the aquatic loss lies in inadequate information on the enormous number of small headwater streams with high CO_2 concentrations. In boreal Sweden, 90% of total stream length is in catchments less than 15 km^2 [11].

Neglecting the aquatic export of terrestrially fixed carbon (via dissolved inorganic carbon (DIC), CH_4, particulate organic carbon (POC), and dissolved organic carbon (DOC)) in landscape carbon budgets results in overestimating net ecosystem exchange by 25% to 70% [12–14]. The active pipe model for inland waters [15] increased estimates of total terrestrial export by two-fold while concluding that CO_2 loss to the atmosphere was necessarily underestimated because small streams were entirely excluded for lack of emission and distribution data [3–7,10]. Subsequently, 'in-stream heterotrophy' was added to the stream portion of the budget [5] but other DIC sources, e.g., DIC-rich groundwaters, are poorly known and therefore excluded. The knowledge gap

between the significant contribution of headwater streams in a basin and the small amount of data about them has been termed *aqua incognita* [11].

All streams in an extensively studied 4th order Swedish boreal catchment were supersaturated in CO_2 [16]. There, CO_2 loss from stream surfaces directly to the atmosphere was 30%–50% of the dissolved carbon (DIC+DOC) exported from the forest (2.9 $gC/m^2/yr$ of 9.8 $gC/m^2/yr$) [17,18]. In an Alaskan headwater stream network, greatest variability and mean fluxes of CO_2 were in the first order streams [19] with 9.0 $gC/m^2/yr$ lost from the entire Yukon River basin [20].

In sub-boreal catchments in Canada [21] and a peat catchment in northeast Scotland [13], CO_2 loss from stream surfaces was 36% and 34% of the dissolved carbon exported from the catchments. These studies noted that gas loss from stream surfaces to the atmosphere is significant, but all neglected the higher CO_2 evasion rates from stream surfaces upstream of their sampling locations. Without good estimates of CO_2 fluxes, ecosystem-scale metabolism calculations also contain this uncertainty and bias. DIC in headwater streams is a net result of a number of processes, including: dissolution of carbonate and weathering of some minerals in soils and bedrock, in-stream biotic respiration and fixation, exchange with atmospheric CO_2, and shallow groundwater input [17,22–25]. Although it is commonly assumed that CO_2 saturation is controlled by mineral weathering and in-stream biotic activity in carbonate systems, boreal forests are, in many cases, characterized by high-DIC shallow groundwaters derived from terrestrially respired organic carbon [8,24].

Here, we focus on silicate bedrock catchments because they constitute 45% of boreal catchments [1] and we avoid the complications of the contribution of significant amounts of DIC from carbonate [26]. Silicate-dominated boreal landscapes contribute significantly to global carbon fluxes [27]. Headwater streams in these catchments have low to moderate pH values and moderate to high concentrations of CO$_2$ that is modern in radiocarbon terms [28,29]. Thus, DIC from shallow groundwater is directly related to soil and root respiration instead of long-term mineral weathering.

In undisturbed, shaded, nutrient-poor, silicate-bedrock, boreal headwater streams, shallow groundwater is the major source of DIC since in-stream respiration is low relative to gas exchange with the atmosphere [30–33]. Furthermore, in silicate terrain, shallow groundwater retains the δ^{13}C value of the DIC input from DOC and soil OC decomposition and exhibits modern radiocarbon ages [28,29] indicating weathering is unimportant at this scale. Thus for small streams of up to a few hundred metres length in this landscape, soil and root respiration is the key δ^{13}C-DIC source.

Degassing of CO$_2$ from these streams causes the δ^{13}C-DIC to increase due to well known equilibrium isotopic fractionation between CO$_2$, HCO$_3^-$, and CO$_3^{2-}$ and during CO$_2$ loss to the atmosphere — since the δ^{13}C- CO$_2$ value is less than the bulk δ^{13}C-DIC value, the loss of CO$_2$ will cause the remaining δ^{13}C-DIC value to increase [34,35]. Additionally, since CO$_2$ loss does not affect carbonate alkalinity, there is a concomitant increase in pH as degassing occurs along the stream [36]. This CO$_2$ loss also includes CO$_2$ lost as groundwater transits the riparian zone adjacent to the stream since these DIC and δ^{13}C-DIC changes are indistinguishable from those in the stream proper. Recent work presented a moderately complex modelled formulation of the degassing effects on δ^{13}C-DIC and focused on several French streams [35].

At a much broader level, we can use the characteristic degassing trajectories of decreasing DIC vs increasing δ^{13}C-DIC to estimate (1) how far along the degassing curve a particular sampling site in a stream is and (2) how much CO$_2$ loss there must have been upstream of the sampling site. This gives us the opportunity to use discrete samples from a stream to estimate the upstream CO$_2$ loss without direct knowledge of the DIC concentration of the groundwater end-member. Since groundwater δ^{13}C-DIC can be easily constrained based on C3 plants and soil organic matter formation [22,28,37] in silicate-dominated catchments, the average groundwater DIC concentration can then be determined as a result of the modelling process. Discrete samples are available from the mouths of streams where whole-lake mass balances have been completed [38], along stream networks [16,39], and potentially from archived samples and data sets [40]. Because only in-stream samples are needed, this technique makes it possible to cover large catchment areas. Logistically, headwater stream CO$_2$ fluxes can be rapidly assessed without the large investment required to study only one catchment in detail.

Given the (1) poor knowledge of the extent of headwater stream surface area (lengths and widths [11,24], but see recent methods using digital elevation models [18,20] and branching theory [41]) and (2) narrow constraint on δ^{13}C-DIC in groundwater, we suggest these small streams can be studied with archived and new samples. We place the results in a context of landscape-scale degassing trajectories where δ^{13}C-DIC of groundwater, stream, and small lakes all differ. We focus on improving CO$_2$ loss estimates from headwater stream surfaces in two catchments: (1)

Harp Lake, Canada where stream CO$_2$ loss is situated in a catchment C budget and (2) Krycklan, Sweden where stream CO$_2$ losses are higher than previously estimated.

Materials and Methods

Site description

Two field sites of contrasting vegetation and location were selected: Harp Lake catchment, Canada (45°22′ N, 79°08′ W) and Krycklan catchment, Sweden (64°14′ N, 19°50′ E). Three headwater streams in the Harp Lake catchment were studied. All are underlain by the gneissic bedrock of the Canadian Shield [42] with mixed forests of sugar maple (*Acer saccharum*), beech (*Fagus grandifolia*), yellow birch (*Betula alleghaniensis*), white pine (*Pinus strobus*), and aspen (*Populous tremuloides*). Harp Lake catchment receives 1033 mm/yr precipitation. Mean annual air temperature is 5°C. Stream catchments ranged from 3.7 km^2 to 21.7 km^2 with stream lengths from 170 m to 760 m. All streams were first or second order and catchments had varying amount of wetland cover (<0.3% to 8.5%) [43,44].

Stream samples from around Harp Lake were collected from July 1989 to November 1991 across various flow conditions near the mouth of each stream ($n = 111$). DIC samples were collected in Pyrex culture tubes with polycone caps and analysed colorimetrically as per standard methods in the Ontario Ministry of the Environment lab at Dorset, Ontario, Canada. Samples for δ^{13}C-DIC analysis were collected in 500 mL glass bottles with polycone caps and analysed by standard off-line dual-inlet IRMS techniques. Groundwater was sampled from piezometers near the middle of the Harp 4–21 catchment ($n = 8$) [28,29]. An automated titrator (PC-Titrate Man-Tech Associates) was used to measure pH. Stream temperature was measured in the field. Stream DOC concentrations varied with stream flow with a median concentration of 5.1 mgC/L (range of 1.1 mgC/L and 17.2 mgC/L) and flow-weighted annual average around 10 mgC/L [45,46]. Harp Lake epilimnion was sampled from March 1990 to November 1991 for DIC concentration and δ^{13}C-DIC ($n = 22$).

This work was initially conducted to study the origin, transport, cycling, and fate of organic carbon from soils to DOC and DIC in a soft water catchment by combining δ^{13}C and Δ^{14}C analyses [28,29,42,43,45,46]. DOC turnover rates in streams, lakes, and wetlands are fast, <40 yr, and on the same time scale as acid deposition in the area. There is extensive DOC cycling in upper soil layers and the source of DOC to headwater streams changes seasonally with water table level. Soil CO$_2$ and δ^{13}C- CO$_2$ profiles show characteristic patterns of root respiration, decomposition of SOM and diffusional gradients along with modern radiocarbon ages.

The Krycklan catchment is underlain by metagreywacke bedrock and has forests of Norway spruce (*Picea abies*) and Scots pine (*Pinus sylvestris*), but deciduous trees are commonly found in the riparian zone of larger streams. It receives 600 mm/yr precipitation. Mean annual air temperature is 1°C. Stream catchment areas ranged from 0.03 km^2 to 67 km^2 and stream lengths from 0.02 km to 96.5 km. Streams were first to fourth order and had varying amounts of wetland cover (0% to 40%) [16].

Stream samples were collected in June, August, and November 2006 ($n = 43$). All samples were collected in septum-capped, screw-topped glass vials and analysed via headspace equilibration by gas chromatography or on-line GC-IRMS. Shallow groundwater was sampled from suction lysimeters along a transect parallel to the lateral flow paths towards one of the headwater streams ($n = 12$).

Stream temperature was measured in the field. Typical annual pH range of was 3.7 to 6.3 in headwaters and 5.7 to 7.4 in 4th order streams. First-order-stream DOC concentrations were 5.0 mgC/L to 40.0 mgC/L and in 4th order streams were 5.0 mgC/L to 15.0 mgC/L [47].

Research at Krycklan catchment is focused on integrating water quality, hydrology, and ecology in flowing waters [48]. Some recent work includes characterizing the loss of CO_2 from stream surfaces by stream size and season [16,47]. Streams were always supersaturated in CO_2, greatest in the headwaters, and negatively correlated with pH [16]. Owing to the importance of the gas exchange coefficient in controlling CO_2 loss rates and its requirement for scaling across landscapes, it was independently measured across streams in Krycklan catchment [47]. The source of the excess CO_2 was largely explained as respired carbon being exported from catchment soils [49]. As part of this work, δ^{13}C-DIC values can be used to identify CO_2 degassing, compared with the labour-intensive flux measurements, scaled flux estimates, and to asses the upstream CO_2 loss that is demonstrated to be large and important [18].

Calculations

We built a simple, parsimonious degassing model in Matlab (MathWorks, Natick MA USA) for high-DIC, low-pH, silicate headwater streams. Only DIC concentration, pH, δ^{13}C-DIC and temperature are required to be measured in the stream since all other carbonate species concentrations and δ^{13}C values can be calculated. The model partitioned total DIC into CO_2, HCO_3^-, and CO_3^{2-} according to pH and temperature-dependent acid dissociation constants and equilibrium [50,51] and kinetic [52] fraction factors as summarized by [34]. The calculations here are similar to those employed in CO2sys [53], seacarb [54], and streamCO₂-DEGAS [35] but do not require as many input parameters, many of which are not available for our catchments. In small headwater streams, this simple approach may be

appropriate to survey a large area. Larger, more detailed models may be required for larger and longer streams and rivers, but it becomes more difficult to measure all variables required to ground-truth such models.

Key assumptions to this approach are that streams are nutrient-poor, low pH, with low community metabolic rates relative to stream velocity and gas exchange, and catchments have C3 vegetation, silicate bedrock, with high DIC shallow groundwater reflective of the vegetation and soils. Both Harp Lake catchment [21,28,29,42–46,55] and Krycklan catchment [16,24,47,56–58] meet these assumptions. Both have low nutrient concentrations, pH values, and associated metabolic rates under undisturbed forest canopies. Stream lengths and segments are on the order of hundreds of metres and water travel times are less than an hour. Forests in these catchments contain only C3 vegetation, are sub-boreal and boreal, and are underlain by crystalline silicate bedrock. Groundwaters are acidic and DIC-rich, as outlined below. This approach is generalizable to the plethora of small streams that meet these criteria across the silicate bedrock areas of the sub-boreal and boreal forests such as the headwaters of catchments on the Canadian and Fennoscandian/Baltic Shields. Source code is provided so that additional components can be added to address the complexities of carbon cycling as needed if the basic assumptions for field sites are not met, such as larger streams with longer travel times, large diel temperature variability, the confluence of several stream sections, measured rates of in-stream metabolism, known patterns of groundwater discharge, or the influence of carbonate-rich bedrock following portions of the streamCO₂-DEGAS model [35], which has been used in larger rivers. Further, model sensitivity to variability in input parameters may be easily assessed with Monte Carlo approaches.

The chemical equilibrium calculations can be easily recreated in any modelling language. Since ionic strength of these soft waters is very low (conductivity is typically 15–40 μS), the activity coefficients were assumed to be approaching unity. This time-forward model differs from [35] in that: (a) carbonate dissolution

Table 1. Typical model input and calculated parameters.

| Parameter	Typical Value	Unit	Notes	Citation
Typical model input parameters (Fig. 2 and raw data)				
DIC	1200	μmol/L	Typical measured value	
pH	5.5		Typical measured value	
Temperature	4	°C	Typical measured value	
δ^{13}C-DIC	−26	‰	Typical measured value	
Calculated parameters based on model inputs above				
Alk	103	μeq/L	Carbonate alkalinity held constant	
CO_2	1098	μmol/L	Calculated from DIC, pH, logK_a, logK_b	
CO_{2eq}	25	μmol/L	Calculated from logk_H and $p_{CO_2 atm}$	
ϵ_b	−10.3	‰	CO_2*–HCO_3^-, function of temperature	[34, 50]
ϵ_c	3.3	‰	HCO_3^-–CO_3^{2-}, function of temperature	[34, 52]
ϵ_g	−1.2	‰	CO_2– CO_2, function of temperature	[34, 50]
logK_a	−6.53		CO_2–HCO_3^-, function of temperature	[68]
logK_b	−10.6		HCO_3^-–CO_3^{2-}, function of temperature	[69]
logk_H	−1.18	log(mol/L/atm)	$CO_{2 atm}$– CO_2, function of temperature	[50]
$p_{CO_2 atm}$	380	ppmv	Partial pressure of CO_2 in the atmosphere	
pK_w	14.8		Function of temperature	[70, 71]

doi:10.1371/journal.pone.0101756.t001
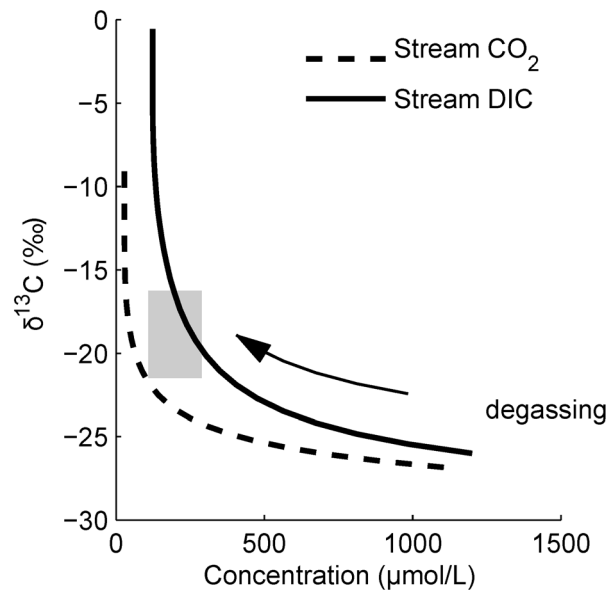
Figure 1. DIC and CO$_2$ degassing trajectories show that as CO$_2$ is lost from streams, δ^{13}C values increase at different rates for DIC and CO$_2$. δ^{13}C-DIC is typically measured, not δ^{13}C- CO$_2$, but the δ^{13}C of both DIC and CO$_2$ during CO$_2$ loss can be modelled using well known isotope fractionation factors. For this example, a typical groundwater end-member was chosen with initial DIC of 1200 μmol/L, δ^{13}C-DIC of -26‰, pH of 5.5, and thus carbonate alkalinity of 103 μC- CO$_2$, but the δ^{13}C of both DIC and CO$_2$ during CO$_2$ loss can be modelled using well known isotope fractionation factors. For this example, a typical groundwater end-member was chosen with initial DIC of 1200 μmol/L, δ^{13}C-DIC of -26‰, pH of 5.5, and thus carbonate alkalinity of 103 μeq/L. In watersheds, variation in the groundwater end-member results in a 'family' of curves with similar trajectories. The grey box represents the 25th and 75th percentiles of DIC and δ^{13}C-DIC collected from three different first- and second-order streams draining into Harp Lake, Ontario, Canada. Samples were collected at the mouth of each stream from July 1989 to November 1991 ($n = 111$). Significant CO$_2$ loss (60% to 80%) must have occurred by the sampling point in each stream in order for the box to fall where it does on the degassing curve.
doi:10.1371/journal.pone.0101756.g001

was not included since our catchments are on silicate bedrock; (b) total alkalinity calculations differ slightly; (c) DIC concentration is the basis for calculations rather than total alkalinity; (d) the model starts with a small plug of shallow groundwater discharged to the surface; (e) groundwater is continuously added to the modelled stream if there are corresponding flow measurements; and (f) the iterative process to find a best fit between measured stream values and modelled results.

Though there is some contribution of organic acids to total alkalinity [59], loss or gain of CO$_2$ does not change organic or carbonate alkalinity. Here we model alkalinity based on the carbonate system since in high-DIC, low-pH waters the main cause of pH change is CO$_2$ loss and assume that the contribution of organic alkalinity to pH is relatively constant and minor.

In practice, to calculate the fraction of CO$_2$ lost by the sampling point in the stream, DIC concentration, pH, and δ^{13}C-DIC measurements in the stream are required. An inverse modelling approach is used as the time-forward model takes initial constrained estimates of groundwater DIC, pH, and known δ^{13}C-DIC, and allows CO$_2$ to degas with time. The resulting values of stream DIC, pH, δ^{13}C-DIC, and δ^{13}C- CO$_2$ with time are outputs. The model was iteratively re-run with Matlab's *fminsearch* function to reduce the sum of squared errors between measured stream DIC, pH, and δ^{13}C-DIC and modelled values. The resulting best-fits then provide the average groundwater DIC concentration and the amount of CO$_2$ that was lost upstream of the sampling point. In this way, an average groundwater DIC concentration can be determined. Additionally, the groundwater δ^{13}C-DIC must be determined but this value is highly constrained by plant and soil δ^{13}C values, as above, and can be confirmed with

a number of piezometers [28,29]. Matlab code to run the model forward and inversely is available from the corresponding author and https://github.com/jjvenky/CO2-from-headwater-streams.

At each time step, a small portion of CO$_2$ was removed from the modelled aquatic system via gas exchange:

$$\frac{dCO_2}{dt} = k \times \left(CO_{2eq} - CO_2 \right) \quad (1)$$

where k is the gas exchange coefficient, CO$_{2eq}$ is the CO$_2$ equilibrium concentration determined with the Henry's constant [50], and CO$_2$ is the solvated CO$_2$ concentration. This necessarily reduced the DIC concentration since:

$$\frac{dDIC}{dt} = \frac{dCO_2}{dt} \quad (2)$$

$$DIC = CO_2 + HCO_3^- + CO_3^{2-} \quad (3)$$

The remaining DIC was then re-apportioned to its constituent species by determining the pH (as H$^+$) required to hold the carbonate-based alkalinity constant [36,60]:

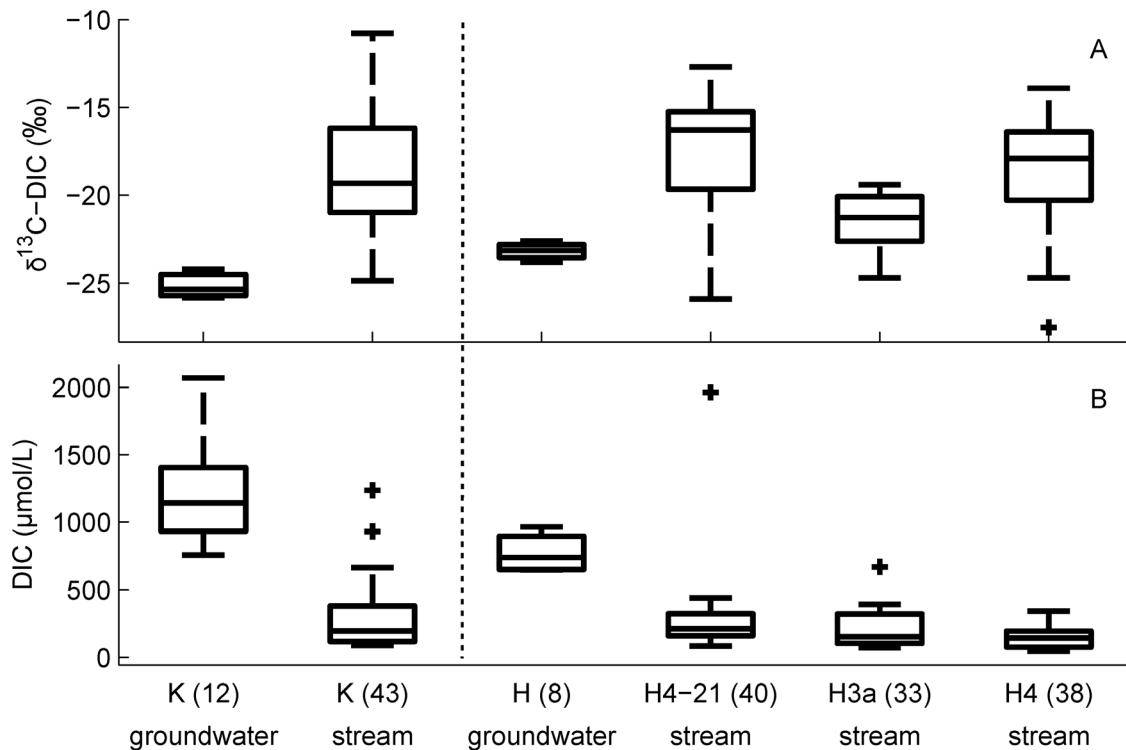$$H^+ = HCO_3^- + 2 \times CO_3^{2-} + OH^- - Alkalinity \quad (4)$$

Figure 2. Groundwater and stream (a) δ^{13}C-DIC values and (b) DIC concentrations from headwater catchments in Sweden (left) and Canada (right). Groundwater and stream data are from the headwater stream network in Krycklan catchment, Sweden (K) and three first- or second-order streams draining into Harp Lake, Ontario, Canada (H with stream numbers; [43,44]). The boxes represent 25th and 75th percentiles, mid-line the median, whiskers the most extreme datum not outside 1.5 × inter-quartile range (IRQ), and + the data outside 1.5 × IQR. Number of samples is indicated in parentheses. At these two sites where we have both groundwater and stream data, there is a clear increase in δ^{13}C-DIC values from groundwater to stream sampling points along with a large decrease in DIC concentration.
doi:10.1371/journal.pone.0101756.g002

The δ^{13}C portion of the model employed well-known temperature-dependent isotopic fractionation factors between DIC species, and solvated CO_2 and atmospheric CO_2 [34]: at 4°C, these are kinetic gas exchange fractionation (-1.3‰) since the k for $^{13}CO_2$ is slightly slower than for $^{12}CO_2$, equilibrium fractionation (-1.2‰) between atmospheric CO_2 and solvated CO_2, CO_2–HCO_3^- fractionation (-10.3‰), and HCO_3^-–CO_3^{2-} fractionation ($+3.3$‰). At each time step, the δ^{13}C value of each species was calculated. Typical values of input parameters and calculated parameters are summarized in Table 1.

The effects of continuous groundwater input to the modelled stream that significantly changes the stream volume over the reach of interest can also be included by adding an amount of water with known or estimated initial groundwater values (DIC, δ^{13}C-DIC, pH, alkalinity) at each time step. The amount can be determined by stream length and discharge measured at the catchment outlet or as the difference in flow between two sites. This comprised an additional input parameter used during best-fit modelling of the H4-21 data since this is a small first-order stream, the stream length is known, and the discharge was measured at the stream mouth along with DIC, δ^{13}C-DIC, and pH. Here, groundwater input was assumed to be constant down the reach. In each case, the CO_2 lost was multiplied by the measured daily discharge and reported relative to the catchment area.

Permissions

Headwater streams in the Harp Lake catchment were studied under the auspices of pre-existing Ontario Ministry of the Environment research program. The Krycklan catchment is a part of the Svartberget LTER site run by the Swedish University of Agricultural Sciences and the area is developed for scientific purposes. Specific permissions for these activities were not required. No endangered or protected species were involved in either site.

Results and Discussion

As CO_2 is initially lost from a stream, there is little associated change in δ^{13}C-DIC (Fig. 1). Only after about half of the DIC has been lost is there an observable change of about 2‰ in δ^{13}C-DIC. In streams where measured δ^{13}C-DIC values are significantly different than shallow groundwater, a large amount of CO_2 must have already been lost from the stream by the time the sample was collected (Fig. 1). Thus, CO_2 flux measurements obtained with data from an individual sampling site where the δ^{13}C-DIC value is several per mille greater than the groundwater δ^{13}C-DIC value must underestimate stream and catchment CO_2 loss rates since the stream surface with higher CO_2 concentrations and higher flux rates is upstream of such a sampling site. The degree of underestimation needs to be better quantified because these results suggest that net ecosystem exchange and C storage may be lower than assumed in boreal and sub-boreal ecozones.

We applied these ideas to a suite of headwater stream data from Krycklan catchment in Sweden and Harp Lake in Canada for which both groundwater and stream measurements were available. Stream DIC concentrations were lower and δ^{13}C-DIC and
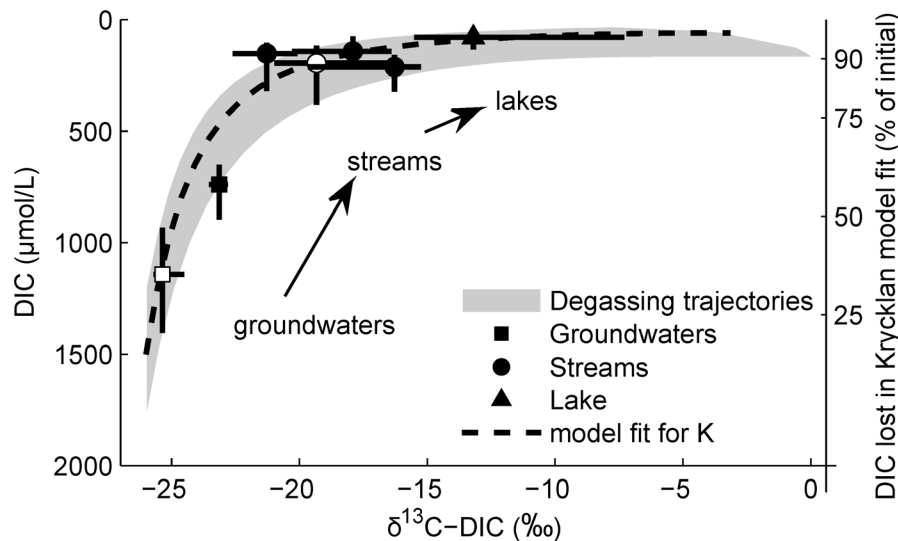
Figure 3. Typical DIC and CO$_2$ degassing trajectories (grey band) show that small initial increases in δ^{13}C-DIC values signify large losses in CO$_2$ from groundwater to streams. The δ^{13}C progress along this trajectory is a natural result of CO$_2$ degassing, not other processes (e.g., primary production, mineral weathering, etc.). The grey band represents the combined trajectories of degassing curves with a combination of initial DIC concentrations (1200 to 1800 μmol/L), δ^{13}C-DIC (-26‰) and pH values (4.0 to 5.5). The grey band also describes the landscape-scale trajectory of DIC concentrations and δ^{13}C-DIC values from shallow groundwater discharging into headwater streams and degassing while flowing downhill to small lakes. Groundwater, stream, and lake data from the two study sites are displayed as 25th and 75th percentiles (lines) with medians (symbols). Harp Lake data are from the epilimnion from March 1990 to November 1991 ($n=22$). The line represents the degassing trajectory that was fit to the median of the Krycklan (open symbols) dataset. The secondary y-axis indicates the amount of DIC lost along the degassing model fit for the Krycklan site.

pH values greater than their respective groundwater values in both catchments (Fig. 2). The range of δ^{13}C-DIC in shallow groundwater, -26‰ to -24‰ is tightly constrained by the narrow range of δ^{13}C in C3 plants and soil. This is comparable to measured δ^{13}C-DOC values [28] so in-stream respiration would produce DIC with the same δ^{13}C-DIC value as shallow groundwater. Surface water was allowed to lose CO$_2$ via gas exchange and the chemical and isotopic equilibria were adjusted accordingly (see Methods).

There are many groundwater discharge patterns possible. In small streams, the difference in discharge measured at two locations may be the only way to estimate groundwater inputs. As such, it may be difficult to parameterize [43]. In a stream network in Alaska, high resolution CO$_2$ and discharge data suggest variable and varying groundwater inputs [19] along the lengths of the streams. The net effect of groundwater input to small streams is to increase stream DIC concentration, reduce the δ^{13}C-DIC value, decrease pH, and make the stream appear closer to the initial shallow groundwater values (Figs 1 and 2).

While shallow groundwaters in boreal forest catchments vary, to some extent in DIC concentration, δ^{13}C-DIC, pH, and temperature, the effect of changing these variables does not alter the fundamental relationship between δ^{13}C-DIC and DIC during CO$_2$ degassing. Increased initial DIC concentration, lower pH, and lower alkalinity cause the sigmoid-like relationship to approach its plateau δ^{13}C-DIC value more quickly and thus requires a greater loss of CO$_2$ before δ^{13}C-DIC values will increase appreciably. This is demonstrated in the range of landscape-scale degassing trajectories (grey area in Fig. 3). This range is akin to a sensitivity analysis by confirming the shape of the DIC vs δ^{13}C-DIC relationship across a wide range of DIC concentrations and pH values. Buffered groundwaters discharging

into headwater streams exhibit a shallower curve than acidic, poorly buffered waters. The degassing trajectories in DIC vs δ^{13}C-DIC space describe the CO$_2$ loss from groundwaters to streams and ultimately to headwater lakes as decreasing DIC, increasing δ^{13}C-DIC, and increasing pH (Fig. 3).

Scaling-up fluxes estimated via these methods to catchment- and landscape-scale requires areas or lengths of headwater streams, catchment areas, or groundwater discharge areas. Here, we avoid using stream length and surface area, parameters not easily obtained in headwater catchments, but see [18,20], and instead report stream losses relative to their catchment area. In this manner, the CO$_2$ loss from aquatic surfaces is easily compared in the same units used to assess net ecosystem exchange and productivity at the catchment scale.

One of the study catchments, a small first-order upland stream in a sub-boreal temperate forest (H4-21) [61], lost a median 15 mgC/m^2/d between its source and mouth ($n=21$, range 3–100 mgC/m^2/d). This is a flux-weighted loss of 5 gC/m^2/yr (range 1–40 gC/m^2/yr) and is comparable to the annual DOC export (1–8 gC/m^2/yr) from the catchment (Fig. 4). It is also around 10% of catchment net CO$_2$ uptake [62]. Unlike DOC, this CO$_2$ loss occurred from the small stream surface and was lost directly to the atmosphere before the stream outlet. Furthermore, this CO$_2$ loss would not have been quantified at the mouth of the stream using conventional measures of CO$_2$ and DIC fluxes [38]. Previous estimates of CO$_2$ flux rates from the mouth of Harp Lake streams [21] are much smaller than our estimate. This highlights the fact that measured CO$_2$ concentrations decline down the length of streams and CO$_2$ loss is underestimated when it is calculated from the sampling points of lowest measured concentrations.
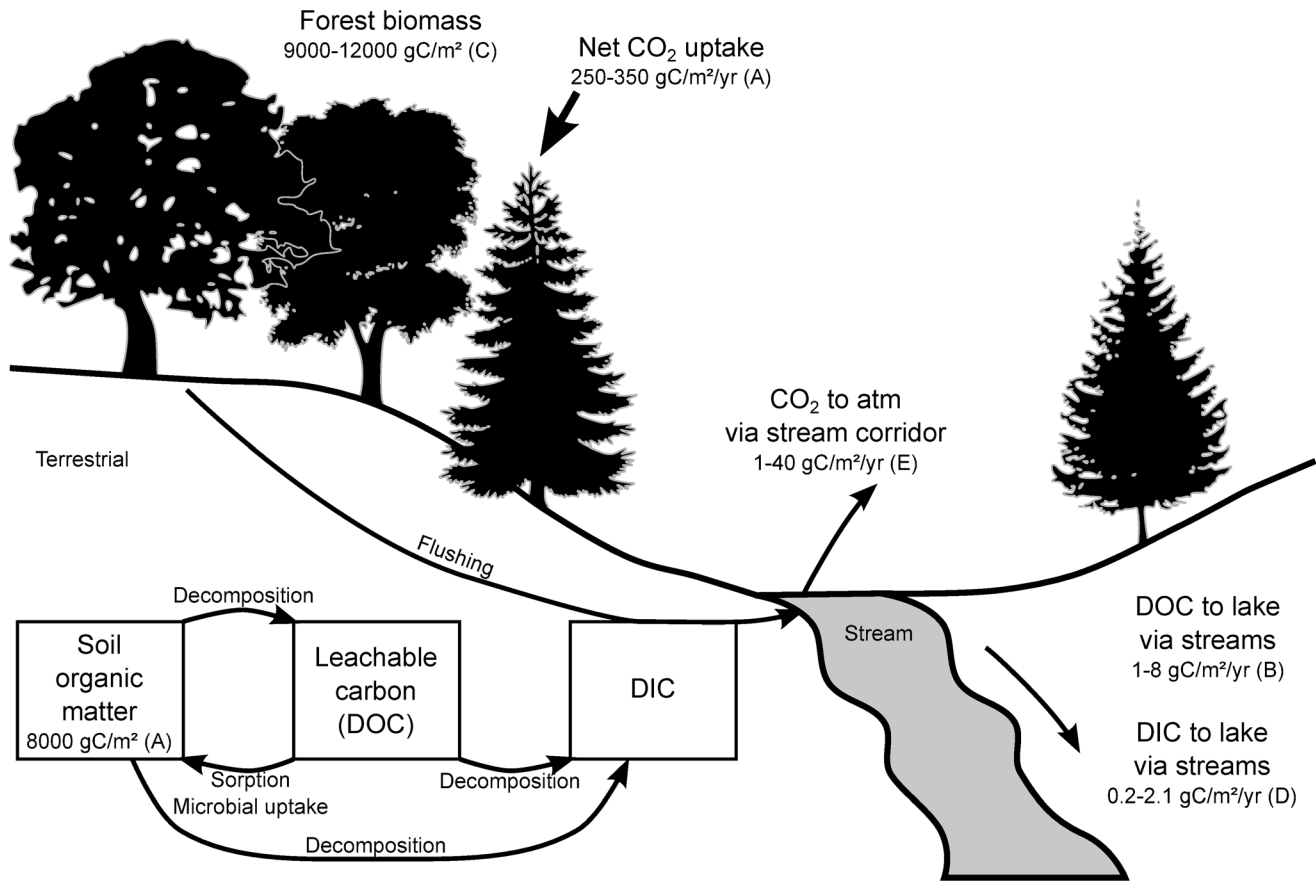
Figure 4. Schematic drawing showing the size of some of the organic carbon pools, carbon fluxes, and important processes affecting DOC, DIC and CO$_2$ in terrestrial catchments and aquatic surfaces. Decomposition from soil organic matter includes microbial exudates. Production of DOC, decomposition, microbial uptake/sorption, root respiration, mineral weathering, and flushing are competing processes affecting the export of DOC and DIC via streams in forested catchments. Loss of CO$_2$ directly to the atmosphere from the surfaces in the stream corridor can exceed the sum of DIC and DOC export to downstream lakes. Total losses of carbon lost by CO$_2$ emissions and dissolved carbon export (DIC+DOC) can be important relative to net CO$_2$ uptake by forests from the atmosphere. All rates are per catchment area. (Figure after [42]; A. [62]; B. [38]; C. range for boreal and temperature forests [66]; D. [38,67]; E. this study.)
doi:10.1371/journal.pone.0101756.g004

The other study catchment, a typical stream network in Krycklan, Sweden [18], lost upwards of 13–28 mgC/m^2/d. This estimate is necessarily larger than the CO$_2$ concentration based estimated loss of 5.0 gC/m^2/yr. It is also larger than the DOC+DIC export of 4.6 gC/m^2/yr and is 14–29% of estimated the net ecosystem exchange of 96 gC/m^2/yr [18].

This method of using measured in-stream δ^{13}C-DIC values shows that the CO$_2$ loss from aquatic surfaces in these boreal and sub-boreal catchments is large and under-estimated. The areal flux rates we present for Harp Lake and Krycklan catchments are similar to those arrived at using much more intensive sampling and different sets of assumptions. This supports the use of a parsimonious model in similar locations. The pattern of measured δ^{13}C-DIC values in small streams being much higher than expected shallow groundwater δ^{13}C-DIC values, is present in other datasets [23,25,40] and indicates there is a large flux of CO$_2$ from headwater streams that has not been included in our continental carbon budgets.

With a measurement at one point in a small stream, the CO$_2$ loss can be estimated by this δ^{13}C approach for a certain distance upstream. In H4-21, using a first-order-loss-rate expression ($3U/k$,

where U is stream velocity and k is gas transfer coefficient, [63]), typical gas transfer coefficients (7–25 d^{-1}, [21]), typical measured mean discharge (1–20 L/s), typical cross-sectional areas (250–1000 cm^2), the upstream distance over which the CO$_2$ degassing occurred was 375–1375 m.

Grab samples can be used to demonstrate the degree of degassing that has occurred at a given location with a parsimonious model — the simplicity of the DIC–alkalinity–pH–δ^{13}C-DIC calculations means this idea can be easily incorporated into site-specific calculations. Further, stream CO$_2$ loss, normalized to catchment area, is likely to be larger than CO$_2$ loss from lake surfaces since lake CO$_2$ loss is typically less than that half of the DOC input [5,38,64].

Headwater stream CO$_2$ loss is a reduction in the net ecosystem productivity of boreal and sub-boreal forests. It is a globally important flux since boreal and sub-boreal ecozones are so large [1]. Here, we have shown it can be easily estimated at the catchment scale by combining δ^{13}C-DIC measurements with in-stream and groundwater samples. Ultimately, C loss via stream degassing may be required to be integrated into northern hemispheric CO$_2$ uptake and loss rates [2,7,18,65].

Author Contributions

Conceived and designed the experiments: JJV SLS MBW. Performed the experiments: JJV SLS MBW. Analyzed the data: JJV SLS MBW. Contributed reagents/materials/analysis tools: JJV SLS MBW. Wrote the paper: JJV SLS MBW.

References

1. FAO (2001) Global forest resources assessment 2000. Technical report, FAO. URL http://www.fao.org/DOCREP/004/Y1997E/Y1997E00.HTM.
2. Stephens BB, Gurney KR, Tans PP, Sweeney C, Peters W, et al. (2007) Weak northern and strong tropical land carbon uptake from vertical profiles of atmospheric CO₂. Science 316: 1732–1735.
3. Battin TJ, Kaplan LA, Findlay S, Hopkinson CS, Marti E, et al. (2008) Biophysical controls on organic carbon fluxes in fluvial networks. Nature Geoscience 1: 95–100.
4. Battin TJ, Luyssaert S, Kaplan LA, Aufdenkampe AK, Richter A, et al. (2009) The boundless carbon cycle. Nature Geoscience 2: 598–600.
5. Tranvik LJ, Downing JA, Cotner JB, Loiselle SA, Striegl RG, et al. (2009) Lakes and reservoirs as regulators of carbon cycling and climate. Limnology and Oceanography 54: 2298–2314.
6. Aufdenkampe AK, Mayorga E, Raymond PA, Melack JM, Doney SC, et al. (2011) Riverine coupling of biogeochemical cycles between land, oceans, and atmosphere. Frontiers in Ecology and the Environment 9: 53–60.
7. Raymond PA, Hartmann J, Lauerwald R, Sobek S, McDonald C, et al. (2013) Global carbon dioxide emissions from inland waters. Nature 503: 355–359.
8. Humborg C, Morth CM, Sundbom M, Borg H, Blenckner T, et al. (2010) CO₂ supersaturation along the aquatic conduit in Swedish watersheds as constrained by terrestrial respiration, aquatic respiration and weathering. Global Change Biology 16: 1966–1978.
9. de Wit HA, Austnes K, Dalsgaard L, Hylen G (2013) A carbon budget of Norway: integration of terrestrial and aquatic C fluxes. Geophysical Research Abstracts 15: EGU2013–5158.
10. Butman D, Raymond PA (2011) Significant efflux of carbon dioxide from streams and rivers in the United States. Nature Geoscience 4: 839–842.
11. Bishop K, Buffam I, Erlandsson M, Folster J, Laudon H, et al. (2008) Aqua incognita: the unknown headwaters. Hydrological Processes 22: 1239–1242.
12. Kling GW, Kipphut GW, Miller MC (2001) Arctic lakes and streams as gas conduits to the atmosphere: implications for tundra carbon budgets. Science 251: 298–301.
13. Hope D, Palmer SM, Billett MF, Dawson JJC (2001) Carbon dioxide and methane evasion from a temperate peatland stream. Limnology and Oceanography 46: 847–857.
14. Richey JE, Melack JM, Aufdenkampe AK, Ballester VM, Hess LL (2002) Outgassing from Amazonian rivers and wetlands as a large tropical source of atmospheric CO₂. Nature 416: 617–620.
15. Cole JJ, Prairie YT, Caraco NF, McDowell WH, Tranvik LJ, et al. (2007) Plumbing the global carbon cycle: Integrating inland waters into the terrestrial carbon budget. Ecosystems 10: 171–184.
16. Wallin M, Buffam I, Öquist MG, Laudon H, Bishop K (2010) Temporal and spatial variability of dissolved inorganic carbon in a boreal stream network: Concentrations and downstream fluxes. Journal of Geophysical Research: Biogeosciences 115: G02014.
17. Öquist MG, Wallin M, Seibert J, Bishop K, Laudon H (2009) Dissolved inorganic carbon export across the soil/stream interface and its fate in a boreal headwater stream. Environmental Science & Technology 43: 7364–7369.
18. Wallin MB, Grabs T, Buffam I, Laudon H, Ågren A, et al. (2013) Evasion of CO₂ from streams – the dominant component of the carbon export through the aquatic conduit in a boreal landscape. Global Change Biology 19: 785–797.
19. Crawford JT, Striegl RG, Wickland KP, Dornblaser MM, Stanley EH (2013) Emissions of carbon dioxide and methane from a headwater stream network of interior Alaska. Journal of Geophysical Research: Biogeosciences 118: 482–494.
20. Striegl RG, Dornblaser MM, McDonald CP, Rover JR, Stets EG (2012) Carbon dioxide and methane emissions from the Yukon River system. Global Biogeochemical Cycles 26: GB0E05.
21. Koprivnjak JF, Dillon PJ, Molot LA (2010) Importance of CO₂ evasion from small boreal streams. Global Biogeochemical Cycles 24: GB4003.
22. Palmer SM, Hope D, Billett MF, Dawson JJC, Bryant CL (2001) Sources of organic and inorganic carbon in a headwater stream: Evidence from carbon isotope studies. Biogeochemistry 52: 321–338.
23. Hope D, Palmer SM, Billett MF, Dawson JJC (2004) Variations in dissolved CO₂ and CH₄ in a first-order stream and catchment: an investigation of soil-stream linkages. Hydrological Processes 18: 3255–3275.
24. Jonsson A, Algesten G, Bergstrom AK, Bishop K, Sobek S, et al. (2007) Integrating aquatic carbon fluxes in a boreal catchment carbon budget. Journal of Hydrology 334: 141–150.
25. Doctor DH, Kendall C, Sebestyen SD, Shanley JB, Ote N, et al. (2008) Carbon isotope fractionation of dissolved inorganic carbon (DIC) due to outgassing of carbon dioxide from a headwater stream. Hydrological Processes 22: 2410–2423.
26. Kortelainen P (1993) Content of total organic-carbon in Finnish lakes and its relationship to catchment characteristics. Canadian Journal of Fisheries and Aquatic Sciences 50: 1477–1483.
27. Houghton RA (2003) The contemporary carbon cycle. In: Holland HD, Turekian KK, editors, Treatise on Geochemistry. Volume 8: Biogeochemistry, Elsevier, chapter 8.10.
28. Schiff SL, Aravena R, Trumbore SE, Dillon PJ (1990) Dissolved organic-carbon cycling in forested watersheds — a carbon isotope approach. Water Resources Research 26: 2949–2957.
29. Aravena R, Schiff SL, Trumbore SE, Dillon PJ, Elgood R (1992) Evaluating dissolved inorganic carbon cycling in a forested lake watershed using carbon isotopes. Radiocarbon 34: 636–645.
30. Naiman RJ (1983) The annual pattern and spatial distribution of aquatic oxygen metabolism in boreal forest watersheds. Ecological Monographs 53: 73–94.
31. Lamberti GA, Steinman AD (1997) A comparison of primary production in stream ecosystems. Journal of the North American Benthological Society 16: 95–104.
32. Naiman RJ, Melillo JM, Lock MA, Ford TE, Reice SR (1987) Longitudinal patterns of ecosystem processes and community structure in a sub-arctic river continuum. Ecology 68: 1139–1156.
33. Roberts BJ, Mulholland PJ, Houser AN (2007) Effects of upland disturbance and instream restoration on hydrodynamics and ammonium uptake in headwater streams. Journal of the North American Benthological Society 26: 38–53.
34. Zeebe RE, Wolf-Gladrow D (2001) CO₂ in seawater: equilibrium, kinetics, isotopes. New York: Elsevier.
35. Polsenaere P, Abril G (2012) Modelling CO₂ degassing from small acidic rivers using water pCO₂, DIC and δ^{13}C-DIC data. Geochimica et Cosmochimica Acta 91: 220–239.
36. Di Toro DM (1976) Combining chemical equilibrium and phytoplankton models — a general methodology. In: Canale RP, editor, Modeling Biochemical Processes in Aquatic Ecosystems, Ann Arbor, MI, USA: Ann Arbor Science. pp. 233–255.
37. Cerling TE, Wang Y, Quade J (1993) Expansion of C4 ecosystems as an indicator of global ecological change in the Late Miocene. Nature 361: 344–345.
38. Dillon PJ, Molot LA (1997) Dissolved organic and inorganic carbon mass balances in central Ontario lakes. Biogeochemistry 36: 29–42.
39. Giesler R, Lyon SW, Mörth CM, Karlsson J, Karlsson EM, et al. (2014) Catchment-scale dissolved carbon concentrations and export estimates across six subarctic streams in northern Sweden. Biogeosciences 11: 525–537.
40. Waldron S, Scott EM, Soulsby C (2007) Stable isotope analysis reveals lower-order river dissolved inorganic carbon pools are highly dynamic. Environmental Science & Technology 41: 6156–6162.
41. Downing JA, Cole JJ, Duarte CA, Middelburg JJ, Melack JM, et al. (2012) Global abundance and size distribution of streams and rivers. Inland Waters 2: 229–236.
42. Schiff SL, Aravena R, Trumbore SE, Hinton MJ, Elgood R, et al. (1997) Export of DOC from forested catchments on the precambrian shield of central ontario: Clues from ^{13}C and ^{14}C. Biogeochemistry 36: 43–65.
43. Hinton MJ (1998) The role of groundwater flow in streamflow generation within two small forested watersheds of the Canadian Shield. Ph.D. thesis, University of Waterloo.
44. Dillon PJ, Molot LA, Scheider WA (1991) Phosphorus and nitrogen export from forested stream catchments in central Ontario. Journal of Environmental Quality 20: 857–864.
45. Hinton MJ, Schiff SL, English MC (1997) The significance of storms for the concentration and export of dissolved organic carbon from two Precambrian Shield catchments. Biogeochemistry 36: 67–88.
46. Hinton MJ, Schiff SL, English MC (1998) Sources and flowpaths of dissolved organic carbon during storms in two forested watersheds of the Precambrian Shield. Biogeochemistry 41: 175–197.
47. Wallin MB, Öquist MG, Buffam I, Billett MF, Nisell J, et al. (2011) Spatiotemporal variability of the gas transfer coefficient (K_{CO_2}) in boreal streams: Implications for large scale estimates of CO₂ evasion. Global Biogeochemical Cycles 25: GB3025.

48. Laudon H, Taberman I, Ågren A, Futter M, Ottosson-Löfvenius M, et al. (2013) The Krycklan Catchment Study — a flagship infrastructure for hydrology, biogeochemistry, and climate research in the boreal landscape. Water Resources Research 49: 7154–7158.

49. Wallin M (2011) Evasion of CO$_2$ from Streams: Quantifying a Carbon Component of the Aquatic Conduit in the Boreal Landscape. Ph.D. thesis, Swedish University of Agricultural Sciences. URL http://urn.kb.se/resolve?urn = urn:nbn:se:slu:epsilon-3150.

50. Mook WG, Bommerso JC, Staverman WH (1974) Carbon isotope fractionation between dissolved bicarbonate and gaseous carbon-dioxide. Earth and Planetary Science Letters 22: 169–176.

51. Vogel JC, Grootes PM, Mook WG (1970) Isotopic fractionation between gaseous and dissolved carbon dioxide. Zeitschrift für Physik 230: 225–238.

52. Zhang J, Quay PD, Wilbur DO (1995) Carbon-isotope fractionation during gas-water exchange and dissolution of CO$_2$. Geochimica et Cosmochimica Acta 59: 107–114.

53. van Heuven S, Pierrot D, Rae JWB, Lewis E, Wallace DWR (2011). MATLAB program developed for CO$_2$ system calculations. doi:10.3334/CDIAC/otg. CO2SYS_MATLAB_v1.1. ORNL/CDIAC-105b. Carbon Dioxide Information Analysis Center, Oak Ridge National Laboratory, U.S. Department of Energy, Oak Ridge, Tennessee.

54. Lavigne H, Epitalon JM, Gattuso JP (2014) seacarb: seawater carbonate chemistry with R. URL http://CRAN.R-project.org/package = seacarb.R package version 3.0.

55. Devito KJ, Dillon PJ, Lazerte BD (1989) Phosphorus and nitrogen retention in five Precambrian shield wetlands. Biogeochemistry 8: 185–204.

56. Berggren M, Laudon H, Jonsson A, Jansson M (2010) Nutrient constraints on metabolism affect the temperature regulation of aquatic bacterial growth efficiency. Microbial Ecology 60: 894–902.

57. Grabs T, Bishop K, Laudon H, Lyon SW, Seibert J (2012) Riparian zone hydrology and soil water total organic carbon (TOC): implications for spatial variability and upscaling of lateral riparian TOC exports. Biogeosciences 9: 3901–3916.

58. Kuglerová L, Jansson R, Ågren A, Laudon H, Malm-Renöfält B (2014) Groundwater discharge creates hotspots of riparian plant species richness in a boreal forest stream network. Ecology 95: 715–725.

59. Herczeg AL, Hesslein RH (1984) Determination of hydrogen-ion concentration in softwater lakes using carbon-dioxide equilibria. Geochimica et Cosmochimica Acta 48: 837–845.

60. Choi J, Hulseapple SM, Conklin MH, Harvey JW (1998) Modeling CO$_2$ degassing and pH in a stream-aquifer system. Journal of Hydrology 209: 297–310.

61. Hinton MJ, Schiff SL, English MC (1993) Physical properties governing groundwater flow in a glacial till catchment. Journal of Hydrology 142: 229–249.

62. Trumbore SE, Schiff SL, Aravena R, Elgood R (1992) Sources and transformation of dissolved organic carbon in the Harp Lake forested catchment: The role of soils. Radiocarbon 34: 626–635.

63. Chapra SC, Di Toro DM (1991) Delta method for estimating primary production, respiration, and reaeration in streams. Journal of Environmental Engineering 117: 640–655.

64. Hesslein RH, Broecker WS, Quay PD, Schindler DW (1980) Whole-lake radiocarbon experiment in an oligotrophic lake at the Experimental Lakes Area, Northwestern Ontario. Canadian Journal of Fisheries and Aquatic Sciences 37: 454–463.

65. Peters W, Jacobson AR, Sweeney C, Andrews AE, Conway TJ, et al. (2007) An atmospheric perspective on North American carbon dioxide exchange: CarbonTracker. Proceedings of the National Academy of Sciences of the United States of America 104: 18925–18930.

66. Hudson RJM, Gherini SA, Goldstein RA (1994) Modeling the global carbon-cycle: Nitrogen-fertilization of the terrestrial biosphere and the missing CO$_2$ sink. Global Biogeochemical Cycles 8: 307–333.

67. Molot LA, Dillon PJ (1997) Photolytic regulation of dissolved organic carbon in northern lakes. Global Biogeochemical Cycles 11: 357–365.

68. Harned HS, Davis R Jr (1943) The ionization constant of carbonic acid in water and the solubility of carbon dioxide in water and aqueous salt solutions from 0 to 50°. Journal of the American Chemical Society 65: 2030–2037.

69. Harned HS, Scholes SR Jr (1941) The ionization constant of HCO$_3^-$ from 0 to 50°. Journal of the American Chemical Society 63: 1706–1709.

70. Dickson AG, Millero FJ (1987) A comparison of the equilibrium-constants for the dissociation of carbonic-acid in seawater media. Deep-Sea Research Part A – Oceanographic Research Papers 34: 1733–1743.

71. Millero FJ (1995) Thermodynamics of the carbon-dioxide system in the oceans. Geochimica et Cosmochimica Acta 59: 661–677.